SCATTERING BY DIELECTRIC ARRAYS ANALYSIS USING THE EXTENDED METHOD OF AUXILIARY SOURCES EMAS IN CONJUNCTION WITH GLOBAL AND PARTIAL COUPLING

Hichem Naamen and Taoufik Aguili
Ecole nationale d'ingénieurs de Tunis
Département Technologie de l'information et de communications
Tunis, Tunisia

Abstract

The paper understudy develop an extended version of the method of auxiliary sources EMAS in the purpose of modeling the scattering response by finite arrays constituted by conducting or dielectric infinite cylinders. The suitable boundary conditions assorted with the judicious decomposed domains guide to the computation of the backscattering cross section. The global electromagnetic coupling between the cylinders is also integrated in the algorithm.

The coupling modeled by the mutual satisfaction of the boundary conditions involves the continuity of the total tangential field components and focuses on the collocation points of every cylinder.

The partial coupling model implements the coupling only between neighboring cylinders. Thus, the linear system matrix is fully simplified, entraining a significant decrease in the computational cost and memory requirements.

According to the global and partial coupling, the numerical results (RCS, pattern field) reveal satisfying agreement with references.

Keywords: *Extended method of auxiliary sources (EMAS), electromagnetic scattering, Global coupling, Partial coupling, Dielectric array...*

1. Introduction

A well-known fact is that the metallic periodic assemblies have been broadly used in microwave, millimeter wave, and optical systems as filters [1, 2], frequency selective surfaces [3, 4], substrate of antennas [5, 6], beam splitters, and mirrors [7], etc. Moreover, the electromagnetic waves scattered by grating are very useful in terms of their exploitation as spectrum analyzers, polarizers, open mesh reflectors [8], etc. The classical method of auxiliary sources MAS is a meshless numerical technique used to solve electromagnetic boundary problems in free space [9]. The electromagnetic fields within each domain are expressed as a linear combination of analytical solutions of Helmholtz equation. These particular solutions constitute the base of auxiliary sources placed on the auxiliary contour surrounded by the physical one [10]. Thus, we have to distribute these auxiliary sources around the physical contour so that the exterior ones generate the interior fields and the outer ones produce the inner fields; thus, two bases must be chosen per dielectric infinite cylinder. Particularly, the method of auxiliary sources is used to solve problems involving one scatterer.

We extend the MAS technique by subdividing the array in a finite number of different scatterers. Each one acts according to the distributed auxiliary sources around its boundary. The extended method of auxiliary sources EMAS is applied directly to the model coupling between different, infinite, and parallel dielectric cylinders illuminated by a TM monochromatic plane wave.

The global coupling implements the fact that every cylinder of the finite array interacts with all the different cylinders; this is modeled by the mutual satisfaction of the boundary conditions just on the collocation points of every cylinder. These boundary conditions lead to a linear system, with a completely filled matrix entraining a difficult computation and having as solution the amplitudes and phases of scattered fields [11].

In order to decrease the computational cost, we suppose that every cylinder is only coupled with the adjacent ones. The mathematical calculus shows that the global matrix is fully simplified and the implementation code realized justifies the low computational cost achieved by this approximation.

Numerical results (RCS, pattern field) reveal good agreement with references.

By the end of the paper, we have the numerical results which justify the technique as well as the possibility to apply it to macro arrays (or to the other parts of the physical problems involving many mutual interactions….).

An $e^{j\omega t}$ time convention is assumed and suppressed throughout the paper.

2. Extended Method of Auxiliary Sources Formulation

2.1. Global coupling

A transverse magnetic to z-axis monochromatic plane wave illuminates under the φ_{inc} incidence a finite two dimensional array of K.L infinite, dielectric and circular cylinders positioned in the xOy plane and Oz directed (Fig.1).

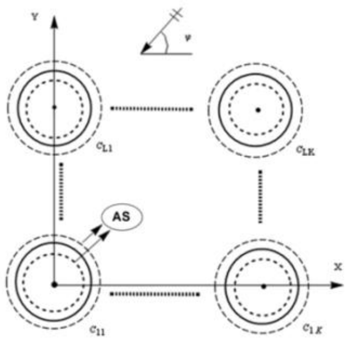

Figure. 1 Finite array geometry of K.L dielectric cylinders.

The incident transverse electric electromagnetic wave has electric and magnetic field expressed as:

$$E_z^{inc}(x,y) = E_0 \exp\{j(k_0(x\cos\varphi_{inc} + y\sin\varphi_{inc}))\}\hat{z} \tag{1}$$

$$H^{inc}(x,y) = -\frac{E_0}{Z_0}(\hat{x}\sin\varphi_{inc} - \hat{y}\cos\varphi_{inc})\exp\{j(k_0(x\cos\varphi_{inc} + y\sin\varphi_{inc}))\} \tag{2}$$

Here, $\hat{z}$ denotes the unit vector in the z-direction and k_0 the free space wave number and Z_0 the free space impedance; since the incident electric field is z-directed and independent of z under the assumption that cylinders are located on the xOy plane, we deduce that the electric scattered field is z-directed too, therefore, it reduces the scattering problem to a two-dimensional one.

For every dielectric cylinder, two bases of auxiliary sources are regularly distributed along the auxiliary contours situated inside and outside the boundary and surrounded by the physical contours, on which the collocation points are positioned.

An inner auxiliary source $(x_{i,j}^{n,in}, y_{i,j}^{n,in})$ indexed by "n" on the $C_{i,j}$ cylinder produces electric and magnetic field expressed as:

$$E_{i,j}^{n,in}(x,y) = -(k_{(0)}Z_{(0)}/4)H_0^{(2)}[k_0 R_{i,j}^{n,in}]I_{(i,j)}^{n,in}\vec{z} \tag{3}$$

$$H_{(i,j)x}^{n,in} = (k_{(0)}(y_{i,j}^{n,in} - y)/4jR_i^l)H_1^{(2)}[k_0 R_i^l]I_{(i,j)}^{n,in} \tag{4}$$

$$H_{(i,j)y}^{n,in} = (k_{(0)}(x - x_{i,j}^{n,in})/4jR_{i,j}^{n,in})H_1^{(2)}[k_0 R_{i,j}^{n,in}]I_{(i,j)}^{n,in} \tag{5}$$

$$R_{i,j}^{n,in} = \sqrt{\left(x - x_{i,j}^{n,in}\right)^2 + \left(y - y_{i,j}^{n,in}\right)^2} \tag{6}$$

Where, $H_0^{(2)}[.]$ represents the second kind Hankel function of the zero order and $I_{i,j}^{n,in}$ shows the complex currents attributed to the n^{th} inner auxiliary source of $C_{i,j}$.

Alternatively, an outer auxiliary source $(x_{i,j}^{n,out}, y_{i,j}^{n,out})$ on the $C_{i,j}$ cylinder produces the electric and magnetic fields expressed as:

$$E_{i,j}^{n,out}(x,y) = -(k_{(i,j)}Z_{(i,j)}/4)H_0^{(2)}[k_{(i,j)}R_{i,j}^{n,out}]I_{(i,j)}^{n,out}\vec{z} \tag{7}$$

$$H_{(i,j)x}^{n,out} = (k_{(i,j)}(y_{i,j}^{n,out} - y)/4jR_{i,j}^{n,out})H_1^{(2)}[k_{(i,j)}R_{i,j}^{n,out}]I_{(i,j)}^{n,out} \tag{8}$$

$$H_{(i,j)y}^{n,out} = (k_{(i,j)}(x - x_{i,j}^{n,out})/4jR_{i,j}^{n,out})H_1^{(2)}[k_{(i,j)}R_{i,j}^{n,out}]I_{(i,j)}^{n,out} \tag{9}$$

According to the standard impedance boundary condition (SIBC), the tangential components of the total electric and magnetic fields must be continuous across the boundary, then for an arbitrary dielectric infinite cylinder $C_{i,j}$ [12]:

$$n_{i,j} \wedge E_{i,j}^{i,j,out} = n_{i,j} \wedge \left(\sum_{p=1}^{p=K} \sum_{q=1}^{q=L} E_{i,j}^{p,q,in} + E_{i,j}^{inc} \right) \tag{10}$$

$$n_{i,j} \wedge H_{i,j}^{i,j,out} = n_{i,j} \wedge \left(\sum_{p=1}^{p=K} \sum_{q=1}^{q=L} H_{i,j}^{p,q,in} + H_{i,j}^{inc} \right) \tag{11}$$

Where $n_{i,j}$ is the outgoing normal vector at the collocation point m of the $C_{i,j}$ cylinder.

Applying these boundary conditions on every dielectric cylinder, we obtain a linear system of 2N.K.L equations and:

$$E_{i,j}^{i,j,out} = \sum_{p=1}^{p=K} \sum_{q=1}^{q=L} E_{i,j}^{p,q,in} + E_{i,j}^{inc} \tag{12}$$

$$n_{i,j} \wedge H_{i,j}^{i,j,out} = n_{i,j} \wedge \left(\sum_{p=1}^{p=K} \sum_{q=1}^{q=L} H_{i,j}^{p,q,in} + H_{i,j}^{inc} \right) \tag{13}$$

$E_{i,j}^{p,q,in}$ Is the total electric field generated by all the inner auxiliary sources of the $C_{p,q}$ cylinder and acting on the $C_{i,j}$ collocation points.

$E_{i,j}^{inc}$ Is the incident electric field on the $C_{i,j}$ cylinder. The linear system (12) serves to indicate that the electric field on each collocation point takes into account the contribution of all the inner auxiliary sources presented in the array. This is certainly true if we assume that for every cylinder, the number of auxiliary sources N is equal to the number of collocation points M. Let us develop the electric boundary condition by substituting every term by its expansion on the adequate auxiliary basis. If we consider a collocation point m on the cylinder $C_{i,j}$, then the following expressions are obtained:

$$E^{inc}_{z,(i,j)}(x,y) = E_0 \exp\{j(k_0(x^{m,inc}_{i,j} cos\varphi_{inc} + y^{m,inc}_{i,j} sin\varphi_{inc}))\}\hat{z} \quad (14)$$

$$E^{i,j,out}_{i,j} = \sum_{n=1}^{n=N} (-(k_{(i,j)} Z_{(i,j)}/4) H^{(2)}_0 [k_{(i,j)} R^{n,out}_{i,j}] I^{n,out}_{(i,j)}) \quad (15)$$

$$E^{p,q,in}_{i,j} = \sum_{n=1}^{n=N} (-(k_{(0)} Z_{(0)}/4) H^{(2)}_0 [k_0 R^{(p,q),n,in}_{i,j}] I^{n,in}_{(p,q)}) \quad (16)$$

$R^{(p,q),n,in}_{i,j}$ Represents the distance between the n^{th} auxiliary source of the $C_{p,q}$ cylinder, and the considered collocation point on $C_{i,j}$.
$Z_{(i,j)}$ Is the intrinsic impedance of $C_{i,j}$ dielectric medium.
After some calculus manipulations and simplifications, the expanded form of the electric condition is:

$$\sum_{p=1}^{p=K} \sum_{q=1}^{q=L} \sum_{n=1}^{n=N} ((k_{(0)} Z_{(0)}/4) H^{(2)}_0 [k_0 R^{(p,q),n,in}_{i,j}] I^{n,in}_{(p,q)}) - \sum_{n=1}^{n=N} ((k_{(i,j)} Z_{(i,j)} /4) H^{(2)}_0 [k_{(i,j)} R^{n,out}_{i,j}] I^{n,out}_{(i,j)}) = E^{inc}_{i,j} \quad (17)$$

Similarly, the second system equation traducing the magnetic boundary condition yields to:

$$n_{(i,j)x} . H^{i,j,out}_{(i,j)y} - n_{(i,j)y} . H^{i,j,out}_{(i,j)x} = (n_{(i,j)x} (\sum_{p=1}^{p=K} \sum_{q=1}^{q=L} H^{p,q,in}_{(i,j)y})) - (n_{(i,j)y} (\sum_{p=1}^{p=K} \sum_{q=1}^{q=L} H^{p,q,in}_{(i,j)x})) + (n_{(i,j)x} . H^{inc}_{(i,j)y} - n_{(i,j)y} . H^{inc}_{(i,j)x}) \quad (18)$$

Taking into account the fact that the elementary magnetic fields radiated by the current filaments are:

$$H^{i,j,out}_{(i,j)x} = \sum_{n=1}^{n=N} (k_{(i,j)} (y^{n,out}_{i,j} - y)/4jR^{n,out}_{i,j}) H^{(2)}_1 [k_{(i,j)} R^{n,out}_{i,j}] I^{n,out}_{(i,j)} \quad (19)$$

$$H^{i,j,out}_{(i,j)y} = \sum_{n=1}^{n=N} (k_{(i,j)} (x - x^{n,out}_{i,j})/4jR^{n,out}_{i,j}) H^{(2)}_1 [k_{(i,j)} R^{n,out}_{i,j}] I^{n,out}_{(i,j)} \quad (20)$$

$$H^{p,q,in}_{(i,j)x} = \sum_{n=1}^{n=N} (k_{(0)} (y^{n,in}_{p,q} - y)/4jR^{(p,q),n,in}_{i,j}) H^{(2)}_1 [k_0 R^{(p,q),n,in}_{i,j}] I^{n,in}_{(p,q)} \quad (21)$$

$$H^{p,q,in}_{(i,j)y} = \sum_{n=1}^{n=N} (k_{(0)} (x - x^{n,in}_{p,q})/4jR^{(p,q),n,in}_{i,j}) H^{(2)}_1 [k_0 R^{(p,q),n,in}_{i,j}] I^{n,in}_{(p,q)} \quad (22)$$

The last linear system has a completely filled matrix, under the assumption that every cylinder is electromagnetically coupled with the others.

2.2. Partial coupling:

Obviously, the insertion of zeros in the matrix system reduces the computational cost. This is achieved by neglecting the coupling between far cylinders compared to the nearest ones. If we presume that only the coupling between the eight neighboring cylinders is highlighted, then, the linear system matrix will take the following form:

$$\sum_{p}^{p\pm1} \sum_{q}^{q\pm1} \sum_{n=1}^{n=N} ((k_{(0)} Z_{(0)}/4) H^{(2)}_0 [k_0 R^{(p,q),n,in}_{i,j}] I^{n,in}_{(p,q)}) - \sum_{n=1}^{n=N} ((k_{(i,j)} Z_{(i,j)} /4) H^{(2)}_0 [k_{(i,j)} R^{n,out}_{i,j}] I^{n,out}_{(i,j)}) = E^{inc}_{i,j} \quad (23)$$

$$-(\sum_{p}^{p\pm1} \sum_{q}^{q\pm1} \sum_{n=1}^{n=N} (k_{(0)} H^{(2)}_1 [k_0 R^{(p,q),n,in}_{i,j}]/4jR^{(p,q),n,in}_{i,j})(n_{(i,j)x} (x - x^{n,in}_{p,q}) + n_{(i,j)y} (y - y^{n,in}_{p,q})) I^{n,in}_{(p,q)} + \sum_{n=1}^{n=N} (k_{(i,j)} . H^{(2)}_1 [k_{(i,j)} R^{n,out}_{i,j}]/4jR^{n,out}_{i,j}) (n_{(i,j)x} (x - x^{n,out}_{i,j}) + n_{(i,j)y} (y - y^{n,out}_{i,j})) I^{n,out}_{(i,j)} = n_{(i,j)x} . H^{inc}_{(i,j)y} - n_{(i,j)y} . H^{inc}_{(i,j)x} \quad (24)$$

The matrix will be fully simplified because only eight lines around the diagonal will be different from zero for every block matrix, particularly in the case where every cylinder is coupled with the eight neighboring ones.

3. Numerical Results

This section is reserved for reporting some numerical results obtained by the computer EMAS implementation code to verify the validity and accuracy of the aforementioned numerical model. In the following examples, the permeability is assumed to be that of free space everywhere except for dielectric cylinders.
The spatial distribution of scattered power is characterized by a cross section. This fictitious area is the radar cross section. As far as the 2D structures are concerned, the scattering width is defined as follows:

$$SW = lim_{\rho\to\infty} [2\pi\rho \frac{|E^{sc}|^2}{|E^{inc}|^2}] \quad (25)$$

For specified auxiliary surfaces, the convergence scale and the accuracy of the method are only reliant on the number of auxiliary sources M. According to MAS, the approximate solution of the boundary problem will tend to exact solution as $M \to \infty$. Therefore, the convergence is ensured [13].
The boundary condition error for boundary 1 defined by the ratio of the absolute difference between the tangential electric fields intensity around the considered boundary to the maximum magnitude of the corresponding incident field:

$$\Delta E_{bc} = \frac{\| E^{1,in}_{(1)} + E^{inc}_{(1)} - E^{1,out}_{(1)} \|}{max \| E^{inc}_{(1)} \|} * 100 \quad (26)$$

The accuracy scrutinized involves an optimization between at least two parameters: the auxiliary distance sandwiched between the auxiliary and physical contours and the number of auxiliary sources per basis for one cylinder, thus the convergence will be attained when the boundary condition error will reach the predesigned accuracy by varying the bases dimensions.

The collocation method is utilized and implemented in the algorithm code to reach the maximal conditionality of the obtained algebraic matrix.

3.1. Scattering by conducting cylinders:

In order to fulfill the numerical validation of the EMAS, we firstly consider scattering by conducting cylinders under the TM wave excitation.

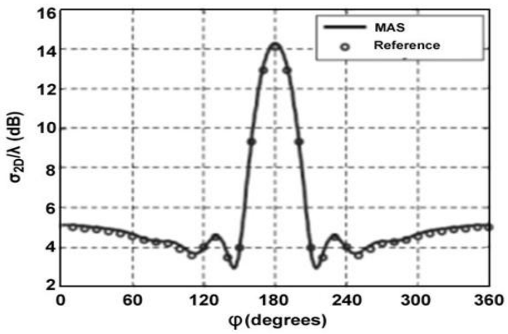

Figure. 2 The echo width results of a TM_z plane wave incident on a PEC cylinder of radius $a = 1\lambda,\ \theta_i = 45°,\ \varphi_i = 90$).

Figure 2 illustrates the normalized bistatic echo width of a TM plane wave incident on a perfectly conducting cylinder of radius $a = 1\lambda$ for an obliquely incident angle $\theta_i = 45°$, $\varphi_i = 90$. It should be pointed out that the results predicted by EMAS and reference [14] are identical.

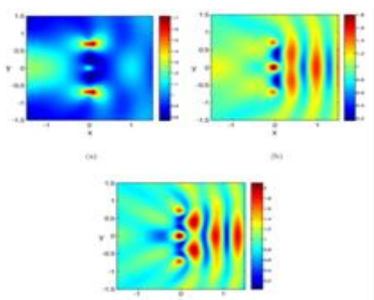

Figure. 3 scattered near field by three conducting cylinders for: (a) $\theta_i = 30°\ et\ \varphi_i = 90°$, (b) $\theta_i = 60°\ et\ \varphi_i = 90°$, (c) $\theta_i = 90°\ et\ \varphi_i = 90°$.

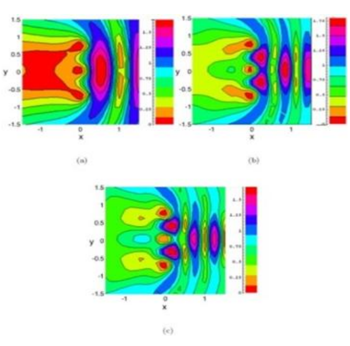

Figure. 4 Near field EMAS results for (a) $\theta_i = 30°\ et\ \varphi_i = 90°$, (b) $\theta_i = 60°\ et\ \varphi_i = 90°$, (c) $\theta_i = 90°\ et\ \varphi_i = 90°$.

Figure 3 shows the scattered near field by three conducting cylinders under the oblique TM plane wave according to [14] and figure 4 represents the numerical results according to the EMAS model. The similarity between the different figures is obvious taking into account the corresponding colors symbolizing each value.

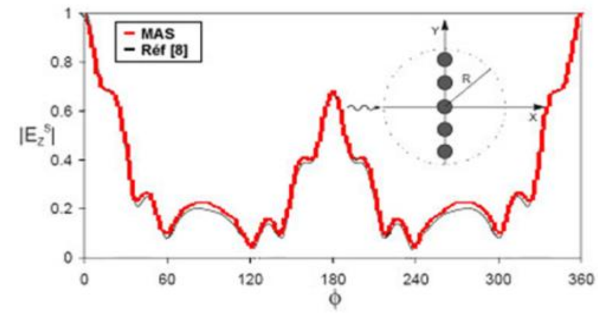

Figure. 5 Scattering by five identical conducting cylinders excited in x-direction with $\rho = 3\lambda$

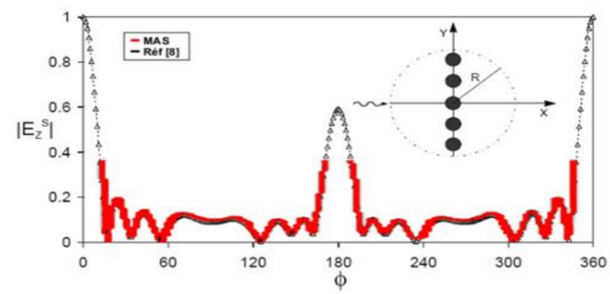

Figure.6 scattering by five identical conducting cylinders excited in x-direction with $\rho = 5\lambda$

Figures 5 and 6 show the scattered field magnitude versus φ direction by a linear array of five conducting cylinders r=0.1 λ in near region $\rho = 3\lambda$ and $\rho = 5\lambda$, where λ is the free space wavelength . The distance between the centers of adjacent cylinders is 0.75λ . For the two outlined distances, the results obtained from global and partial coupling agree very well with [15]. During the implementation, we focused the difference between the axes origins which are used in the reference as well as in the EMAS model.

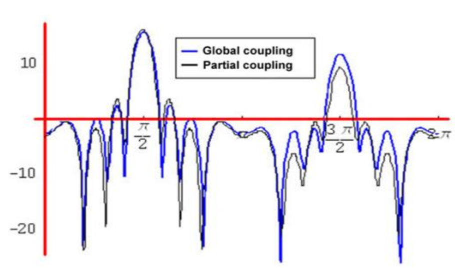

Figure. 7 RCS for five cylinders obtained by the global and partial coupling

Figure 7 reveals the RCS of five cylinders structure [18] realized by applying the global and partial coupling. There is a remarkable similarity between the peak curves and a few lag induced by the auxiliary distances and the number of auxiliary sources choices.

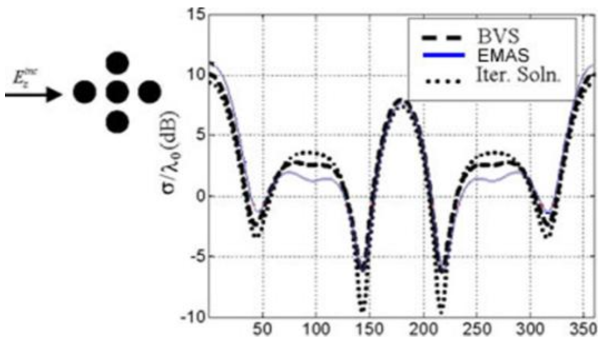

Figure. 8 the bistatic scattering cross section of five perfectly conducting cylinders each of radius = 0.1λ, and their centers are separated by 0.5λ, due to a plane wave incident at $\varphi_0 = 180^\circ$

Figure 8 reveals the RCS of five cylinders structure according to BVS [16] and the EMAS. There is a noticeable similarity between the peak curves and a few lag induced by the auxiliary distances and the number of auxiliary source choices.

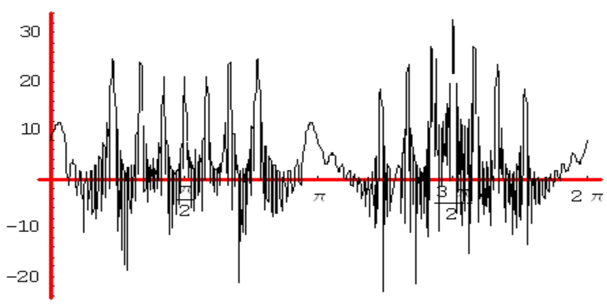

Figure. 9 RCS for 10 conducting cylinders obtained by global coupling.

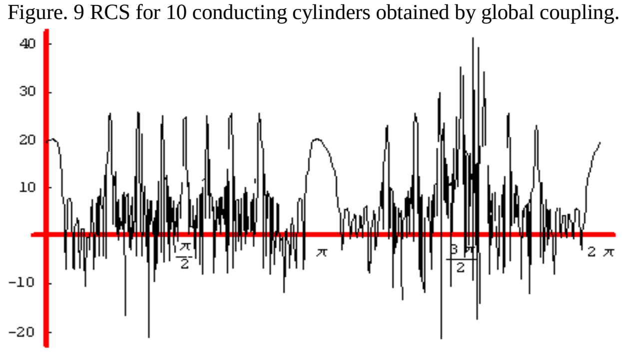

Figure. 10 RCS for 10 conducting cylinders obtained by partial coupling.

Figures 9 and 10 show the RCS of ten conducting cylinders -under the TM plane wave- which have the same geometric parameters as those of figure 5. The numerical results predicted by the EMAS model for global and partial coupling are identical.

3.2. Scattering by dielectric cylinders :

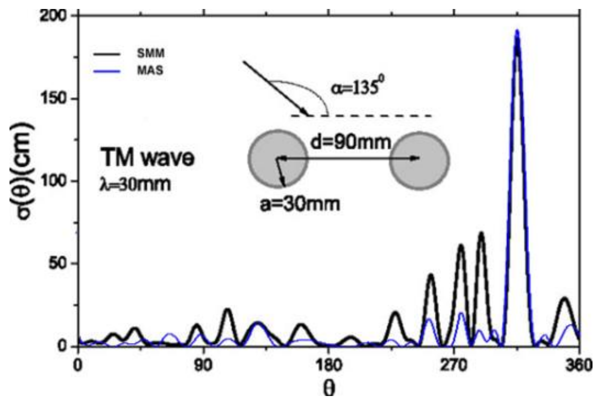

Figure. 11 Bistatic scattering width of two dielectric rods ($\varepsilon r = 2 : 25$).

In order to validate the EMAS model in terms of coupling between dielectric cylinders, figure 11 illustrates the RCS of two dielectric cylinders obtained by the EMAS and the SMM (scattering matrix method) [17], the discrepancy around the great peak comes from the fact that the boundary satisfaction error is less than 1%, therefore, the EMAS modal is more precise than the SMM one.

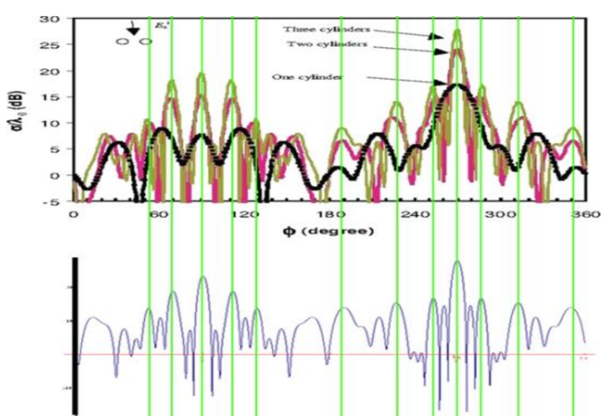

Figure. 12 The scattering cross section of three metamaterial cylinders located on x-axis with $3\lambda_0$ center separation and a $=1\lambda_0$ radius, metamaterial ($\varepsilon_r = -4$, $\mu_r = -1$). The angle of incidence is 90 degrees. The second figure shows the RCS according to MAS for three metamaterials

Figure 12 reveals the RCS of three metamaterial cylinders under the TM plane wave excitation [18]. The peaks in the different curves have the same coordinates with almost no discrepancies.

4. Conclusion

In this paper we have verified that the EMAS model is able to model the plane wave scattering response by an infinite conducting cylinder, for different oblique incidences. The scattering by five and ten conducting cylinders proves that the model is able to control the scattering response and to implement the global and partial electromagnetic coupling with a high accuracy.

The MAS is applied in this paper to model coupling between dielectric and metamaterial cylinders with an acceptable accuracy.

Thus, the EMAS can implement directly the electromagnetic coupling between different scatterers. It can also estimate the scattered field with a predefined accuracy. Moreover, the partial coupling introduced in this paper permits the computational cost decrease by neglecting the electromagnetic coupling between far cylinders.

References

1. S. Peng and G.M. Morris, “Experimental demonstration of resonant anomalies in diffraction from two-dimensional gratings”, Opt. Lett., 21, 549-551, 1996.
2. S. Peng and G.M. Morris, “Resonant scattering two-dimensional gratings”, J. Opt. Soc. Am. A, 13, 993-1005, 1996.
3. D. Sievenpiper, L. Zhang, R.F.J. Broas, N.G. Alexopolous, and E. Yablonovitch, “High-impedance electromagnetic surfaces with a forbidden Frequency band”, IEEE. Trans. Microwave Theory Tech., 47, 2059-2074, 1999.
4. C.M. Horwitz, “A new solar selective surface”, Opt. Comm., 11, 210-212, 1974.
5. V. Veremy, “Superdirective antennas with passive reflectors”, IEEE Antennas and Propagation Magasine, 37(2), 16-26, 1995.
6. C. Simovski and S. He, “Antennas based on modified metallic photonic bandgap structures consisting of capacitively loaded wires”, Microwave Opt. Technol. Lett., 31, 214-221, 2001.
7. R. Ulrich, “Far-infrared properties of metallic mesh and its complementary structure”, Infrared Phys., 7, 37-55, 1967.
8. Victor Twersky, “On scattering of waves by the infinite grating of circular cylinders”, IRE., 737-765, 1962.
9. Fridon shubitidze, Hristos T. Anastassiu and Dimitra I.Kaklamani, “An improved accuracy version of the method of auxiliary sources for computational electromagnetics”, IEEE transactions on antennas and propagation vol52, n1, January 2004.
10. Hristos T Anastassiu et al, “Electromagnetic scattering analysis of coated conductors with edges using the method of auxiliary sources (MAS) in conjunction with the standard impedance boundary condition (SIBC)”, IEEE transactions on antennas and propagation vol50, n1 ,January 2002.
11. Dimitra I. kaklamani and hristos T, “Aspects of the method of auxiliary sources (MAS) in computational electromagnetics”, IEEE transactions on antennas and propagation. vol44, n3, June2002.
12. T.B.A. Senior and Volakis, “Approximate boundary conditions in electromagnetics”.
13. Hristos T.Anastassiu,” Accuracy analysis and optimization of the method of auxiliary sources (MAS) for scattering by a circular cylinder”, IEEE Transactions on Antennas and Propagation, VOL. 52, NO. 6, June 2004.
14. B.H.Henin, A.Z.Elsherbeni, and M. Al Sharkawy, “Oblique incidence plane wave scattering from an array of dielectric cylinders”, Progress in electromagnetic research, PIER 68, 261-279, 2007.
15. M.polewski and Mazur, “Scattering by an array of conducting, lossy dielectric, ferrite and pseudochiral cylinders”, Progress in Electromagnetics Research, PIER 38, 283-310, 2002.
16. M. Al Sharkawy and A. Z. Elsherbeni, “Electromagnetic scattering from parallel chiral cylinders of circular crosssections using an iterative procedure”, Progress in electromagnetics research, PIER 47, 87–110, 2004.
17. Y. J. Zhang, “Fast multipole Accelerated scattering matrix method for multiple scattering of a large number of cylinders”, Progress in electromagnetics research, PIER 72, 105–126, 2007.
18. A. Shooshtari and A. R. Sebak, “Electromagnetic scattering by parallel metamaterial cylinders”, Progress in electromagnetics research, PIER 57, 165–177, 2006